International Telecommunication Union

ITU-R

Radiocommunication Sector of ITU

Report ITU-R SM.2355-0

(06/2015)

Spectrum monitoring evolution

SM Series

Spectrum management

International Telecommunication Union

Foreword

The role of the Radiocommunication Sector is to ensure the rational, equitable, efficient and economical use of the radio-frequency spectrum by all radiocommunication services, including satellite services, and carry out studies without limit of frequency range on the basis of which Recommendations are adopted.

The regulatory and policy functions of the Radiocommunication Sector are performed by World and Regional Radiocommunication Conferences and Radiocommunication Assemblies supported by Study Groups.

Policy on Intellectual Property Right (IPR)

ITU-R policy on IPR is described in the Common Patent Policy for ITU-T/ITU-R/ISO/IEC referenced in Annex 1 of Resolution ITU-R 1. Forms to be used for the submission of patent statements and licensing declarations by patent holders are available from http://www.itu.int/ITU-R/go/patents/en where the Guidelines for Implementation of the Common Patent Policy for ITU-T/ITU-R/ISO/IEC and the ITU-R patent information database can also be found.

Series of ITU-R Reports

(Also available online at http://www.itu.int/publ/R-REP/en)

Series	Title
BO	Satellite delivery
BR	Recording for production, archival and play-out; film for television
BS	Broadcasting service (sound)
BT	Broadcasting service (television)
F	Fixed service
M	Mobile, radiodetermination, amateur and related satellite services
P	Radiowave propagation
RA	Radio astronomy
RS	Remote sensing systems
S	Fixed-satellite service
SA	Space applications and meteorology
SF	Frequency sharing and coordination between fixed-satellite and fixed service systems
SM	**Spectrum management**

***Note**: This ITU-R Report was approved in English by the Study Group under the procedure detailed in Resolution ITU-R 1.*

Electronic Publication
Geneva, 2016

© ITU 2016

All rights reserved. No part of this publication may be reproduced, by any means whatsoever, without written permission of ITU.

REPORT ITU-R SM.2355-0

Spectrum monitoring evolution

(2015)

TABLE OF CONTENTS

Page

1 Introduction 2

2 Detection of weak signal 2

2.1 Locked-in amplifier 2

2.2 Sampled integration 3

2.3 Correlation 4

2.4 Adaptive noise cancelling 6

3 Co-frequency signal separation 7

3.1 Single-channel separation 7

3.2 Multi-channel separation 10

4 Multi-mode location (based on a combination of location technologies) 12

4.1 Angle of arrival 12

4.2 Time difference of arrival 12

4.3 Frequency difference of arrival 12

4.4 Power of arrival 12

4.5 ID-Aided 13

4.6 Gain ration of arrival 13

5 Conclusion 13

Annex 1 – Examples of the application of advanced monitoring techniques 13

A1.1 Correlation application in satellite interference finding 13

A1.2 Strong-signal recovery application in satellite monitoring 17

A1.3 Single-channel ICA application for signal separation 17

A1.4 Spatial spectrum based beam-forming in HF/VHF monitoring 20

A1.5 Multi-channel ICA application for signal separation 22

A1.6 GSM base station geolocation 25

Annex 2 – Examples of the application of combined geolocation 26

A2.1 Hybrid AOA/TDOA 26

A2.2 Hybrid TDOA/GROA 27

1 Introduction

The goal of spectrum management is to maximize spectrum efficiency, minimize interference and eliminate unauthorized and improper use of the spectrum. As the eyes and ears of the spectrum management process, spectrum monitoring is very necessary and important in the management of spectrum resource, radio station, and electromagnetic environment by providing valuable monitoring data, including spectrum occupancy, characteristic of signal, such as field strength, bandwidth, modulation type and location of emitter, etc.

Radiocommunication systems are in constant and rapid evolution. In spectrum utilization aspects it mainly appears to use technologies of adaptive frequency usage, co-frequency multiplexing, wideband access, spread spectrum (direct sequence spread spectrum and frequency hopping), etc. Software-defined radio and cognitive radio systems are typical examples in evolutionary radiocommunication systems. Correspondingly, future spectrum monitoring systems should have capability for monitoring new radiocommunication technologies and systems, such as detection of weak signal, co-frequency signal separation and multi-mode location based on digital signal processing (DSP) and network, etc.

2 Detection of weak signal

It is more and more necessary to improve the sensitivity of monitoring systems to detect low-power-density weak signals because more and more new radiocommunication systems are using lower and lower power, wider and wider bandwidth, higher and higher frequency.

In some circumstances, signals may be weaker than background noise. Consequently, it is difficult to detect and locate illicit low-power-density weak signal using existing monitoring systems with limited sensitivity. Future spectrum monitoring systems should use advanced technology to extract signals from background noise.

Several kinds of technologies on detection of weak signals are listed in the following sections.

2.1 Locked-in amplifier

The sine wave is the most common signal among data communication signals and its amplitude and phase could be estimated by the locked-in amplifier (LIA).

It is assumed that,

$$x(t) = U_S \cos w_0 t + n(t)$$

where:

U_s: amplitude of the sine wave signal

w_0: angular frequency

$n(t)$: background noise.

U_s could be estimated by cross-correlation arithmetic just as the following diagram which is shown in Fig. 1.

FIGURE 1

Diagram of LIA

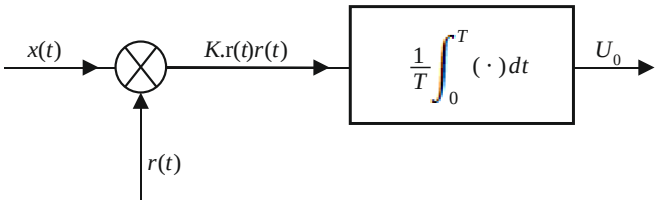

Report SM.2355-0

Here, $r(t)$ is a reference signal with the same frequency as the detected signal $x(t)$ with amplitude U_r and the phase difference φ and K is a constant. Then the output U_o could be described as:

$$U_o = \lim_{T\to\infty}\frac{1}{T}\int_0^T K\left[U_s\cos w_0 t + n(t)\right]\left[U_r\cos(w_0 t+\varphi)\right]dt$$

As the background noise is not correlated to the sine wave signal, the formula can be written as follows:

$$U_0 = \frac{KU_sU_r}{2}\cos\varphi$$

Evidently, $U_o$would get the maximum value and U_s should be measured accurately to great extent if φ is zero, i.e. the reference signal $r(t)$ and the detecting signal $x(t)$ are of the same phase value.

Essentially, the LIA is the application of the cross-correlation technique to some extent.

2.2 Sampled integration

Different from LIA which is suitable for dealing with sine wave signal, the sampled integration technique could be applicable for detection of periodical short-time pulse signal. A diagram of a sampled integration circuit is shown in Fig. 2.

FIGURE 2

Diagram of sampled integration circuit

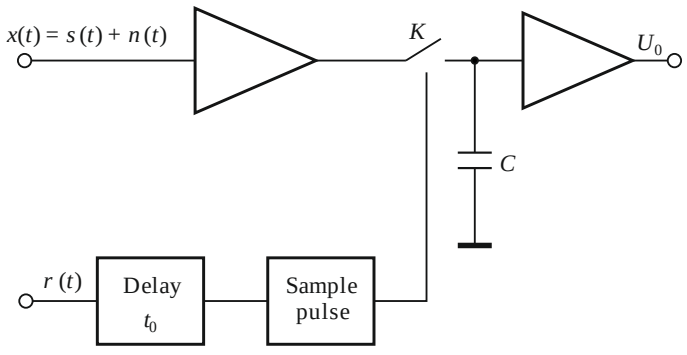

Report SM.2355-02

The reference signal $r(t)$ has the same frequency with the detected signal $x(t)$, which comprises desired signal $s(t)$ and the noise $n(t)$.The $r(t)$ is delayed by t_0 and sample pulse signals are generated to sample $x(t)$ by the switch K. After n times integration and average, the output could be described as follows:

$$u_0 = \frac{1}{n}\sum_{k=0}^{n-1}x(t_0+kT) = \frac{1}{n}\sum_{k=0}^{n-1}s(t_0+kT) + \frac{1}{n}\sum_{k=0}^{n-1}n(t_0+kT)$$

Due to the poor correlation of white noise at different times, the formulas can be obtained as follows:

$$\frac{1}{n}\sum_{k=0}^{n-1} n(t_0 + kT) \approx 0$$

$$u_0 \approx \frac{1}{n}\sum_{k=0}^{n-1} s(t_0 + kT) = s(t_0)$$

The waveforms could be as demonstrated in Fig. 3.

FIGURE 3

Waveforms of signals

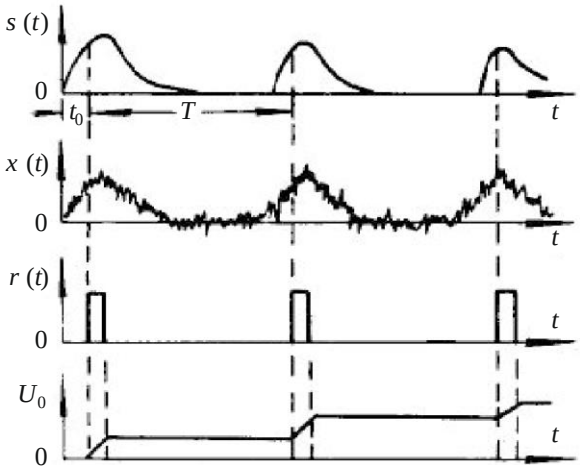

Report SM.2355-03

2.3 Correlation

2.3.1 Cross-correlation

Cross-correlation is a measure of similarity of two waveforms as a function of a time-lag applied to one of them.

It is assumed that

$$x(t) = s_1(t) + n_1(t), \qquad y(t) = s_2(t) + n_2(t)$$

and then

$$\begin{aligned} R_{xy}(\tau) = E[y(t)x(t-\tau)] &= E\{[s_2(t) + n_2(t)][s_1(t-\tau) + n_1(t-\tau)]\} \\ &= R_{s_1 s_2}(\tau) + R_{s_1 n_2}(\tau) + R_{n_1 s_2}(\tau) + R_{n_1 n_2}(\tau) = R_{s_1 s_2}(\tau) \end{aligned}$$

Cross-correlation is applicable for both periodical and non-periodical signals. It is also worth noting that if there is frequency offset between two signals, then the two-dimensional cross-correlation algorithm should be applied. The signal can be modified as

$$x_1(t) = s_1(t) + n_1(t),\ x_2(t) = s_2(t)\exp(j2\pi\Delta f_c t) + n_2(t)$$

where, Δf_c can be denoted as the frequency offset between two signals. The two-dimensional cross-correlation technology can be calculated as

$$R_{xy}(f,\tau) = F\{E[y(t)x(t-\tau)]\}_t = R_{s_1 s_2}(f,\tau)$$

where $F\{\}$ is the Fourier transform with respect to variable τ.

Generally, cross-correlation could generate an outstanding correlation peak with a high SNR. Figure 4 is an example of two-dimensional cross-correlation technique. It is used to estimate the time difference of arrival (TDOA) and frequency difference of arrival (FDOA). It can be clearly seen that an evident peak appears in the Figure. By searching the position of the peak in the time and frequency domain, respectively, the corresponding TDOA and FDOA values can be obtained.

FIGURE 4

Example of two-dimensional cross-correlation

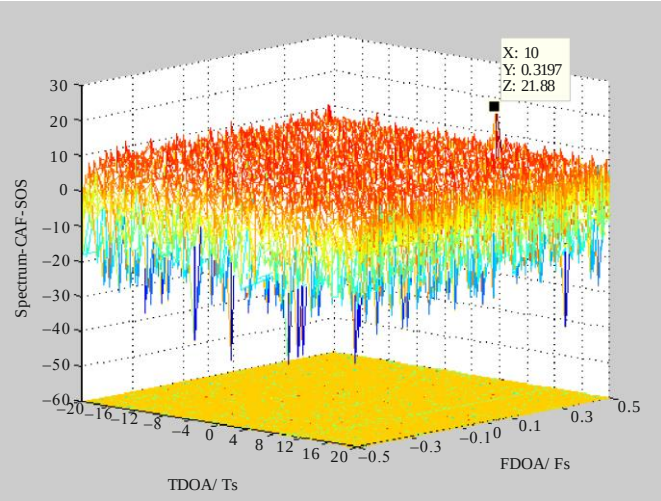

Report SM.2355-0

2.3.2 Auto-correlation

Auto-correlation is the cross-correlation of a signal with itself. Informally, it is the similarity between observations as a function of the time separation between them.

FIGURE 5

Diagram of auto-correlation

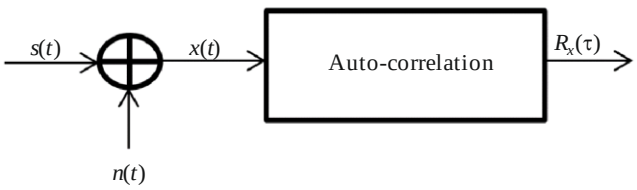

Report SM.2355-05

In Fig. 5, $x(t) = s(t) + n(t)$, $s(t)$ is periodical signal, and $n(t)$ is the noise.

So:

$$R_x(\tau) = E\left[x(t)x(t-\tau)\right] = E\left\{\left[s(t)+n(t)\right]\left[s(t-\tau)+n(t-\tau)\right]\right\}$$
$$= E\left[s(t)s(t-\tau)\right] + E\left[n(t)n(t-\tau)\right] + E\left[s(t)n(t-\tau)\right] + E\left[n(t)s(t-\tau)\right]$$
$$= R_s(\tau) + R_n(\tau) + R_{sn}(\tau) + R_{ns}(\tau)$$

If $s(t)$ and $n(t)$ are not correlated, thus:

$$R_{sn}(\tau) = R_{ns}(\tau) = 0, \text{ and}$$

$$R_X(\tau) = R_S(\tau) + R_n(\tau)$$

If the noise signal $n(t)$ is not periodical and its average value is zero, then:

$$R_n(\tau) = 0 \quad (\text{where} \quad \tau \neq 0)$$

Thus $R_X(\tau) = R_S(\tau)$.

When detecting almost-cyclostationary signals, one modified auto-correlation algorithm, known as "cyclic auto-correlation", can also be applied. Similar to the formula above, it can be expressed as:

$$R_X^{\alpha}(\tau) = E\{x(t)x(t-\tau)\exp(j2\pi\alpha\tau)\}$$
$$= R_S^{\alpha}(\tau) + R_n^{\alpha}(\tau) + R_{sn}^{\alpha}(\tau) + R_{ns}^{\alpha}(\tau)$$

Where α is called cyclic frequency. Similarly, $R_{sn}^{\alpha}(\tau)$ and $R_{ns}^{\alpha}(\tau)$ equals 0, and $R_n^{\alpha}(\tau) = 0$ (where, $\tau \neq 0$ *or* $\alpha \neq 0$).

Thus, $R_x^{\alpha}(\tau) = R_S^{\alpha}(\tau)$.

It is worth noting that the cyclic auto-correlation algorithm is valid for both periodical and non-periodical signals. For periodical signal, we can simply let α = 0, then it is equivalent to the traditional auto-correlation algorithm; while for non-periodical signal, we can let τ = 0, and detect the signal by searching peaks in cyclic frequency domain.

2.4 Adaptive noise cancelling

Adaptive noise cancelling (ANC) obtains the desired signal by subtracting adaptively filtered "reference" noise correlated with the noise contained in the detected signal from the detected signal.

The diagram of adaptive noise cancelling is shown in Fig. 6.

FIGURE 6

Diagram of ANC

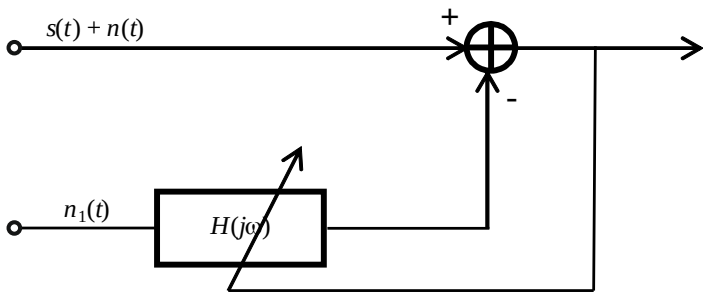

Report SM.2355-0

The reference noise $n_1(t)$ which is correlated with noise $n(t)$ could be processed by the adaptive filter $H(jw)$. The noise $n(t)$ could be restrained, and the output SNR can be improved.

This ANC filter could be designed easily without knowledge or experience of the noise $n(t)$ and the signal $s(t)$, and the filtering effect is equivalent to the Wiener Filter. Because of its advantages, the ANC filter has been widely used to restrain the interference combined with the signals, e.g. the adaptive notch filter.

3 Co-frequency signal separation

More and more new radiocommunication transmitters or systems are sharing limited spectrum resource working at co-frequency in different domains, such as time domain, code domain, spatial domain, etc. For example, many kinds of cellular radiocommunication systems and HF communication systems are working at such a co-frequency model. At the same time most intended or unintended interference cases may happen at overlapping frequencies.

Some advanced radiocommunication systems utilize several co-frequency multiplexing technologies simultaneously. In such cases one spectrum monitoring station may receive some different signals from different transmitters working at same frequency. Consequently, it is difficult to differentiate these co-frequency signals for existing monitoring system with limited function. Future spectrum monitoring systems should use advanced technology to separate signals in different domains.

The technologies of co-frequency signal separation can be divided into two categories: single-channel separation technology and multi-channel separation technology, which are listed in the following sections.

3.1 Single-channel separation

3.1.1 Strong-signal recovery

Strong-signal recovery can be applied to separate the signal from strong linear digital modulated signals, such as PSK and QAM modulated signals. However, this algorithm can only work under the case of two signals, and requires a power ratio of more than 6 dB. The brief diagram of this algorithm is shown in Fig. 7.

FIGURE 7

Diagram of strong-signal recovery

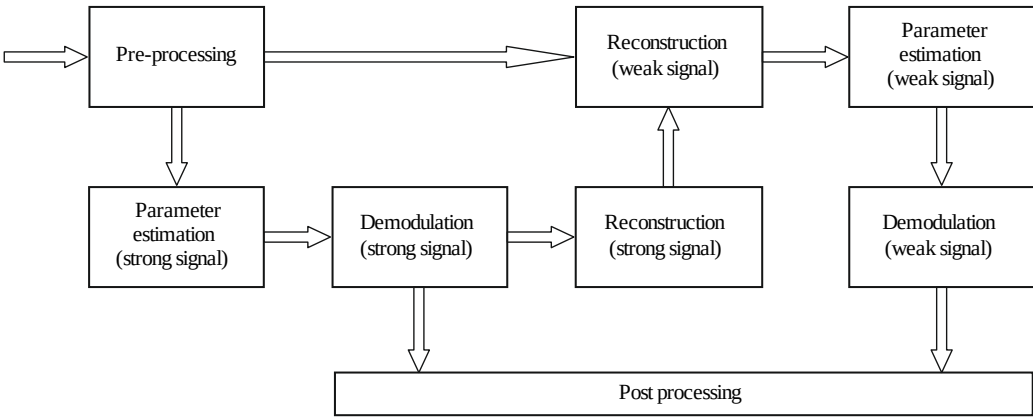

Report SM.2355-0

a) Pre-processing

The main function of this module includes several necessary receiving processing steps, such as filtering, down-conversion, sample rate conversion. Meanwhile, some narrow-band interference cancellation algorithms, such as adaptive notch filtering, which can eliminate the comparable weak signal added on the strong legal signal, can be applied to this module by frequency domain based algorithm.

b) Parameter estimation for strong signal

Several parameters should be estimated for demodulation of strong signals in this module. These parameters include amplitude, carrier frequency, initial phase, modulation rate and type. However, in

most cases, the strong signal is legal. Thus some inherent parameters, such as modulation rate and type, are known to the receiver. So there is no need to estimate these parameters. Only carrier frequency, initial phase and the amplitude are left to be estimated.

c) Demodulation and reconstruction of the strong signal

The conventional demodulation procedure can be applied for the demodulation of strong signals to recover the bit stream sequence. Then the procedure of the strong signal reconstruction can be implemented with prior knowledge of carrier frequency, initial phase, baud rate and modulation type.

d) Reconstruction of the weak signal

After recovery of the strong signal, the weak signal can be reconstructed by adaptive signal cancellation techniques such as least mean square (LMS) and recursive least square (RLS) to eliminate the strong signal from the original mixed signal.

e) Parameters estimation for the weak signal

The required parameters are similar to those mentioned in section b). However, the characteristics of the interfering signal are unknown to the receiver, and thus the necessary parameters, such as baud rate and modulation type, should also be estimated. It is suggested that some robust parameter estimation algorithm should be introduced to eliminate the effect of inaccuracy of the reconstruction.

For instance, the cyclic-spectrum based algorithm can be applied to baud rate estimation, and some high-order statistics based algorithms can be used to design the modulation identification algorithm.

f) Weak signal demodulation

As with the aforementioned statement in section b), the conventional demodulation method can be introduced for the weak signal. Meanwhile, it is suggested that a blind equalization step can be introduced to overcome the inter-symbol interference, which is generated from the inaccuracy of parameter estimation.

3.1.2 Single-channel independent component analysis

Single-channel independent component analysis (ICA) can be applied to separate signal from some digital and analogue modulated signals, such as PSK and AM modulated signals. However, this algorithm can only work under the case of two signals, and an assumption that the channel parameters are constant during the period of signal transmission.

Let us take two BPSK signals for example. The two BPSK signals, with the same carrier frequency and symbol rate, are transmitted through wireless channels and after local oscillator have the form:

$$\beta_1(t) = h_1(t)e^{j(\Delta\omega_1 t+\varphi_1)} \sum_{n=0}^{M} a_n g\left(t - nT - \tau_1\right)$$

and

$$\beta_2(t) = h_2(t)e^{j(\Delta\omega_2 t+\varphi_2)} \sum_{n=0}^{M} b_n g\left(t - nT - \tau_2\right)$$

where $h_1(t)$ and $h_2(t)$ are signal amplitudes polluted by the fading channels, $\Delta\omega_1$ and $\Delta\omega_2$ are carrier frequency offsets, φ_1 and φ_2 are random carrier phases, a_n and b_n are the n-th transmitted symbols which are from the same discrete alphabet $\{-1,1\}$, M is the number of symbols, $g(t)$ are raised-cosine matched filters used against ISI, T is the symbol period, τ_1 and τ_2 are the time delays which satisfy $\tau_1, \tau_2 \in (0,T)$. The mixed signal observed at the receiver can be expressed as:

$$(t) = \beta_1(t) + \beta_2(t) + n(t)$$

where $n(t)$ is an additive white Gaussian noise with power spectrum density $N_0/2$.

If slow-fading channels and perfect carrier frequency synchronization are assumed, the channel gains should then be constant during the period of signals transmitted. We assume the channel gains have the form of $h_j(t)e^{j\varphi_j} = h_j e^{j\varphi_j}$ where j = 1,2. The random channel gains are nuisance in terms of signal detection, but play an important role in signals separation. The observed signal $y(t)$ can be expanded into dual-channel signals by employing the phase-shift version of $y(t)$, as:

$$x_1(t) = h_1 \exp(j\varphi_1) \sum_{n=0}^{M} a_n g_1(t - nT - \tau_1) + h_2 \exp\left[j(\Delta\omega t + \varphi_2)\right] \sum_{n=0}^{M} b_n g_2(t - nT - \tau_2) + n_1(t)$$

and:

$$x_2(t) = h_1 \exp\left[j(\varphi_1 - \theta)\right] \sum_{n=0}^{M} a_n g_1(t - nT - \tau_1) + h_2 \exp\left[j(\Delta\omega t + \varphi_2 - \theta)\right] \sum_{n=0}^{M} b_n g_2(t - nT - \tau_2) + n_2(t)$$

where $\Delta\omega$ is the carrier frequency offset between the co-channel signals, θ is the artificial shifted phase, typically $\theta \in [\pi/4, \pi/2]$, $n_1(t)$ and $n_2(t)$ are assumed to be zero-mean Gaussian noise with variance σ_1^2 and σ_2^2, respectively. By taking the real part of both $x_1(t)$ and $x_2(t)$ the mixing matrix can be obtained as:

$$\mathbf{A} = \begin{bmatrix} h_1 \cos\varphi_1 & h_2 \cos(\Delta\omega t + \varphi_2) \\ h_1 \cos(\varphi_1 - \theta) & h_2 \cos(\Delta\omega t + \varphi_2 - \theta) \end{bmatrix}$$

And the vector of source signals can be expressed as:

$$\mathbf{S} = \begin{bmatrix} s_1 \\ s_2 \end{bmatrix} = \begin{bmatrix} \sum_{n=0}^{M} a_n g(t - nT - \tau_1) \\ \sum_{n=0}^{M} b_n g(t - nT - \tau_2) \end{bmatrix}.$$

If the carrier frequency offset is small and only a short period of observation data is used, then the mixing matrix could be rewritten as:

$$\mathbf{A} = \begin{bmatrix} h_1 \cos(\varphi_1) & h_2 \cos(\varphi_2) \\ h_1 \cos(\varphi_1 - \theta) & h_2 \cos(\varphi_2 - \theta) \end{bmatrix}$$

If $\varphi_1 \neq \varphi_2$, it is not difficult to obtain rank($\mathbf{A}$) = 2. Denote $\boldsymbol{X} = [x_1, x_2]^T$ by the mixing signals vector and obtain a 2 × 2 demixing matrix $\boldsymbol{W} = \mathbf{A}^{-1}$ to recover the sources from $\boldsymbol{X}$ with ICA. The structure of the proposed single-channel ICA algorithm is shown in Fig. 8.

FIGURE 8

Structure of single-channel ICA

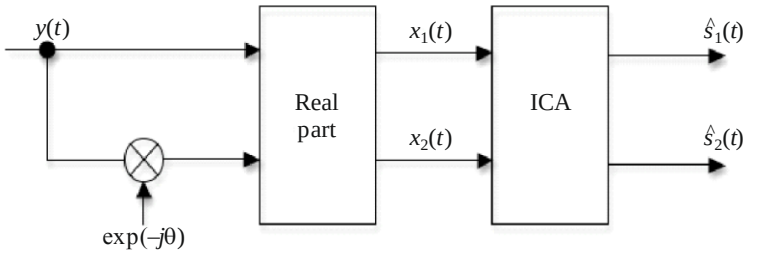

Report SM.2355-08

ICA algorithm can be modelled as the linear combination of instantaneous signals, and the principal is to maximum the independence of the output signals. The blind separation procedure is accomplished by constructing a variety of different de-correlation matrices. ICA does not require any information on the observed signals, but it needs the transmitted signals to satisfy statistical independence. The recovered signal $\hat{\boldsymbol{S}} = [\hat{s}_1, \hat{s}_2]^T$ can be expressed as $\hat{\boldsymbol{S}} = \boldsymbol{W}\boldsymbol{X}$.

3.2 Multi-channel separation

3.2.1 Spatial spectrum based beam-forming

Spatial spectrum based beam-forming can be applied to the scenario of the blind separation of multi-signal, which is also effective under arbitrary modulation type, and can achieve a relatively good performance in low SNR environment. The basic theory can be illustrated as follows:

Assume *P* signals are received by *M* arrays, the received signals can be expressed by matrix $\boldsymbol{X}(t)$ as:

$$\boldsymbol{X}(t)=\begin{bmatrix} 1 & 1 & \cdots & 1 \\ e^{j2\pi d\sin\theta_1/\gamma} & e^{j2\pi d\sin\theta_2/\gamma} & \cdots & e^{j2\pi d\sin\theta_P/\gamma} \\ \vdots & \vdots & \ddots & \vdots \\ e^{j2\pi d(M-1)\sin\theta_1/\gamma} & e^{j2\pi d(M-1)\sin\theta_2/\gamma} & \cdots & e^{j2\pi d(M-1)\sin\theta_P/\gamma} \end{bmatrix} \begin{bmatrix} s_1(t) \\ s_2(t) \\ \vdots \\ s_P(t) \end{bmatrix} + \begin{bmatrix} n_1(t) \\ n_2(t) \\ \vdots \\ n_M(t) \end{bmatrix}$$

where $\{\theta_1,...\theta_P\}$is the direction of each signal respectively, $s_i(t)$ $\{i = 1,2,...P\}$ is denoted as the *P* input signal, $n_i(t)$ $\{i = 1,2,...M\}$ is the corresponding additive white Gaussian noise (AWGN), and γ is the wavelength of the signal.

Then by calculating the correlation matrix:

$$\boldsymbol{R} = E\left(\boldsymbol{X}(t)\boldsymbol{X}^H(t)\right)$$

And, applying an eigenvalue decomposition procedure, a series of eigenvalues and eigenvectors can be obtained. The space of the eigenvalue can be divided into signal subspace of dimension *P*, and noise subspace of dimension *M-P* by the distribution of eigenvalues. The following equation can be easily proven by the orthogonality of the signal and noise subspace as:

$$\boldsymbol{a}(\theta_k)\boldsymbol{G}\boldsymbol{G}^H\boldsymbol{a}^H(\theta_k) = 0$$

where $(\theta_k) = \left[1 e^{j2\pi d\sin\theta_k/\gamma} ... e^{j2\pi d(M-1)\sin\theta_k/\gamma}\right]^T$, $\boldsymbol{G}$ is composed of eigenvectors in noise subspace with dimension $M \times (M\text{-}P)$. Define $\boldsymbol{P}(\theta) = 1/[\boldsymbol{a}(\theta_k)\boldsymbol{G}\boldsymbol{G}^H\boldsymbol{a}^H(\theta_k)]$**,** it is the well-known MUSIC algorithm. The direction of each signal can be estimated by "peak-picking" the series of local maximums of the signals.

If the signal from direction θ_k is to be separated, the coefficients of each array will satisfy the following restriction:

$$\boldsymbol{\omega}^H \boldsymbol{a}(\theta_d)=1, \quad \boldsymbol{\omega}^H \boldsymbol{a}(\theta_i)=0 \ \ (i=1,2,...,M, i\neq d)$$

Varieties of algorithms are designed to solve the problem. One of the most typical and widely used algorithm is the so-called "Capon beam forming", with the principle of minimize the output power. The coefficients can be solved as:

$$\omega_{opt}=\left[R^{-1}a(\theta_k)\right]\Big/\left[a^H(\theta_k)R^{-1}a(\theta_k)\right]$$

It is observed that in estimating the frequencies in an undamped superimposed exponential model better results (in terms of lower mean squared errors) can be obtained by using both the ordinary and the conjugate data than just using the ordinary one for finite length data sequence, although they are asymptotically equivalent. Therefore a modified MUSIC (MMUSIC) algorithm is proposed using both ordinary and conjugate data to estimate DOA of signals. Compared with the MUSIC algorithm, the correlation matrix of the MMUSIC is expressed as

$$\overline{\boldsymbol{R}}=\boldsymbol{R}+\boldsymbol{J}E\left(\overline{\boldsymbol{X}}(t)\overline{\boldsymbol{X}}^H(t)\right)\boldsymbol{J}$$

where, $\overline{\boldsymbol{X}}(t)$ is the conjugate data of $\boldsymbol{X}(t)$, $\boldsymbol{J}$ is the $P \times P$ exchange matrix whose entries all are zero except the one in the $(i,P-i+1)$-th position for $i = 1,2,...P$.

3.2.2 Multi-channel ICA

Multi-channel ICA is widely used in the co-frequency signal separation domain. Compared with the spatial spectrum-based beam-forming algorithm, the ICA algorithm is not sensitive to the relative geometry position of the receiving arrays, and does not need to satisfy the restriction of different direction of arrival, which gives it a better applicability.

The received mixed signal can be expressed as:

$$\boldsymbol{x}(t)=\boldsymbol{A}\boldsymbol{s}(t)+\boldsymbol{n}(t)$$

Where $\boldsymbol{A}$ is the mixed matrix of the $m \times n$ dimension, $\boldsymbol{s}(t) = \{s_1(t),..,s_m(t)\}$ are the original signals, $\boldsymbol{x}(t) = \{x_1(t),..,x_m(t)\}$ is the mixed signal. The separation procedure can be implemented by designing an appropriate non-linear function $\boldsymbol{g}(u)$ and an update algorithm for the matrix W. The basic work flow can be seen in Fig. 9.

FIGURE 9

Structure of multi-channel ICA

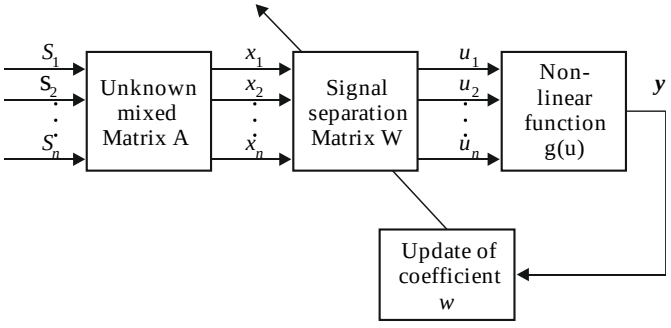

Report SM.2355-0

4 Multi-mode location (based on a combination of location technologies)

Signals in different domains carry related location information. Correspondingly, such location information can be extracted by related technology or computer processing algorithms used in signal location. Digital signal processing (DSP) and networking capability is becoming more and more powerful. Devices based on DSP and networking are becoming more affordable. Spectrum-monitoring systems based on DSP algorithms and network technology can make identification of transmitters with different characteristics working in different domains easier, including amplitude domain, frequency domain, time domain, spatial domain, code domain, etc. Consequently, Multi-mode location technology may be used to locate emitters under different circumstances based on combination of different location technologies, such as AOA (angle of arrival), TDOA (time difference of arrival), FDOA (frequency difference of arrival), POA (power of arrival), and identification data-aided techniques.

4.1 Angle of arrival

Angle of arrival (AOA) is a traditional and popular method of locating a transmitter by determining the direction of propagation of a radio-frequency wave incident on an antenna array under many circumstances. There are many techniques to find the bearing, such as phase interferometer, correlative interferometer, beam forming and space matched filter, subspace techniques, etc. Under certain applications some techniques may be combined in one DF monitoring station used for different purposes. In order to locate a transmitter, it is necessary to combine two or more DF monitoring stations based on AOA technology.

4.2 Time difference of arrival

Time difference of arrival (TDOA) is one promising method of locating a transmitter by estimating the difference in the arrival times of the signal from the source at multiple receivers. TDOA systems offer flexibility in antenna selection and placement as TDOA accuracy is minimally affected by nearby reflectors, and antennas and cables are generally not integral to TDOA receivers. In order to locate a transmitter, it is necessary to combine three or more TDOA systems deployed at different sites. Based on the TDOA values of different pairings of receivers, the position of a transmitter may be determined by utilizing some algorithms, such as non-iterative and iterative algorithms. A more complete discussion of TDOA methods is contained in the Report ITU-R SM.2211-1.

4.3 Frequency difference of arrival

Frequency difference of arrival (FDOA) is one effective method of locating a transmitter in motion or locating a transmitter by a mobile monitoring station, especially an airborne one. Sometimes rapidly selecting signals from different antennas of a monitoring receiving antenna array has similar effectiveness with relative motion between transmitter and monitoring station. This relative motion results in different Doppler shifts, which can be used to calculate transmitter location with knowledge of vector velocities. TDOA and FDOA are sometimes used together to improve location accuracy and the resulting estimates are somewhat independent. By combining TDOA and FDOA measurements, instantaneous geolocation can be performed in two dimensions.

4.4 Power of arrival

Power of arrival (POA) is one economical method of locating a transmitter because POA does not require additional monitoring receiver hardware. The power of a radio signal can be estimated according to propagation models with the knowledge of transmitter power and propagation path, especially used for standardized wireless communication systems. When transmitter power is unknown, it is available to locate a transmitter by calculating PDOA (power difference of arrival) at

pairs of receivers, corresponding to different propagation loss from transmitter to different receivers. In some circumstances it is easy to locate a transmitter when propagation model is simple, e.g. locating an FM broadcasting transmitter when it is in line-of-sight between an FM broadcasting transmitter with fixed monitoring stations.

4.5 ID-Aided

ID-Aided is a more and more important method for locating a transmitter used as a sensor in such a new era of global interconnectedness, especially for pubic radiocommunication networks. Digitalized radiocommunication system includes additional information of user identification, which can be used to locate the transmitter, sometimes accurately, such as longitude and latitude, IP address, etc. It is more effective to locate a transmitter to combine information from monitoring station and matched radiocommunication network database when the transmitter is operating for mobile services. Satellite mobile phone, satellite Internet terminal and handset mobile phone are classical transmitter which could be located by using the ID-Aided method.

4.6 Gain ration of arrival

The gain ratio of arrival (GROA) method is an energy-based passive method that can be used to estimate the positions of the source from the multiple sensors. This method does not require accurate time synchronization between sensors. A particular value of the GROA estimate defines a circle between the two receivers on which the radio transmitter may exist.

5 Conclusion

The techniques and applications for detection of weak signal, co-frequency signal separation and multi-mode location based on DSP and network are briefly described in this Report, including locked-in amplifier, sampled integration, auto-correlation, cross-correlation and adaptive noise cancelling, strong signal recovery, spectrum-based beam-forming, single-channel ICA, multi-channel ICA, FDOA, POA, ID-Aided, and GROA which may be used in future spectrum monitoring under different circumstances.

More advanced spectrum monitoring techniques and applications should be studied for implementation in order to respond to the rapid development of new radiocommunication systems. Examples of some advanced monitoring techniques are found in Annexes 1 and 2.

Annex 1

Examples of the application of advanced monitoring techniques

A1.1 Correlation application in satellite interference finding

In many cases, GSO satellite interference can be located within an ellipse area whose centre is tens of kilometres or farther from the transmitter location.

In the above circumstance, signals from the interfered satellite and adjacent satellite are correlated by the transmitter location systems, and then the TDOA and FDOA data can be generated.

To quickly locate and identify transmitter on the ground is a key issue by spectrum-monitoring stations in many countries or administrations.

The weak signal transmitted by side-lobes of an antenna, which points to GSO satellite, should be detected by equipment. Then we can utilize the cross-correlation technique to improve the sensitivity

of the monitoring system installed on the mobile vehicle. A brief diagram of this application is shown in Fig. A1-1.

FIGURE A1-1

Diagram of cross-correlation application in satellite interference finding

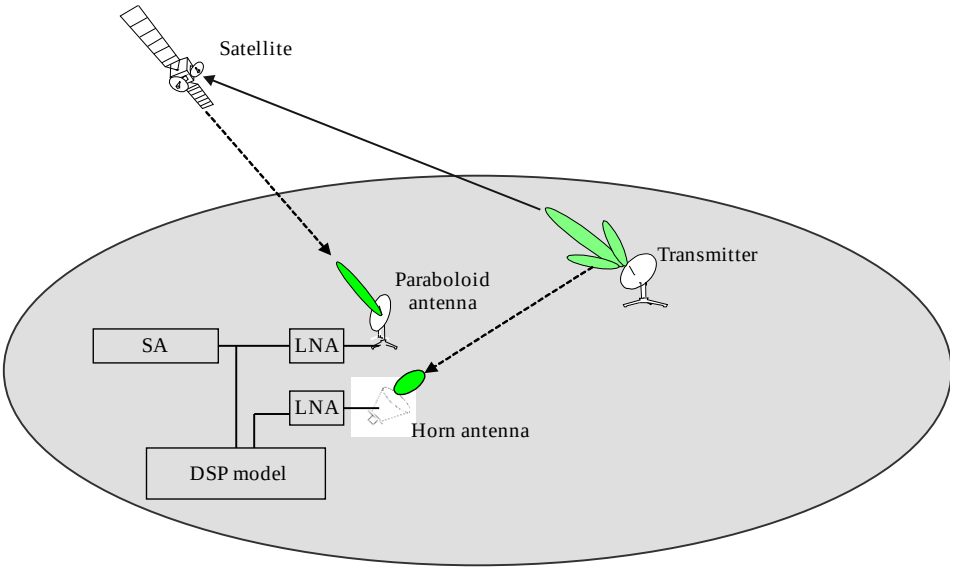

Report SM.2355-A1-0

In this system, cross-correlation arithmetic is utilized in the DSP module to process signals from the satellite by parabolic antenna and from the side-lobe of the earth station antenna by horn antenna or isotropic antenna directly.

The process diagram in the DSP module is described in Fig. A1-2.

FIGURE A1-2

Process diagram in DSP module

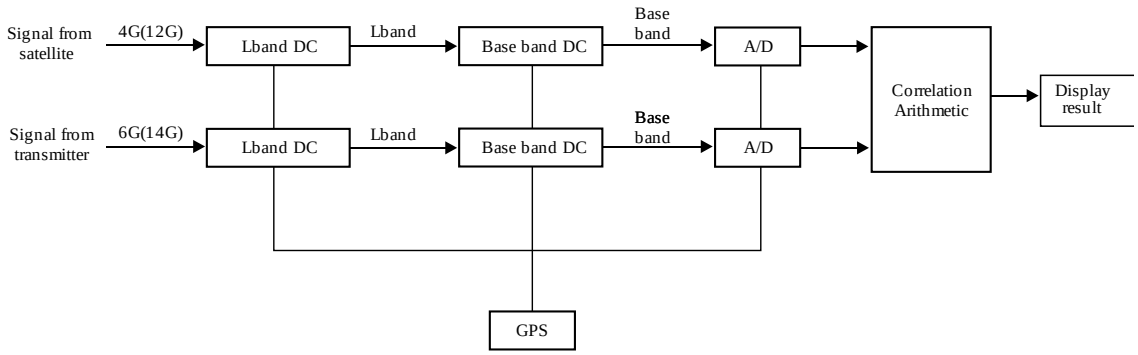

Report SM.2355-A1-0

In the cross-correlation arithmetic, the complex ambiguity function based on a second-order statistics (CAF-SOS) algorithm is used to simultaneously estimate the TDOA and FDOA of signals from satellite and transmitter.

The cross-correlation SNR can be described as follows and each *snr* is a linear value.

$$snr = 2BT * \frac{snr_1 * snr_2}{1 + snr_1 + snr_2}$$

Where 2*BT* is processing gain, if signals are sampled with the Nyquist rate and *N* is the sample point number, we shall get $2BT = N$. The snr_1 represents the snr of signal from satellite, and snr_2 represents the snr of the signal from transmitter. In common cases, *snr* is no less than 20 dB.

If *snr* is equal to 10 dB, the relation between *snr* and snr_2 can be described as in Fig. A1-3.

FIGURE A1-3

Relation between *snr* and snr_2 when snr_1 = 10 dB

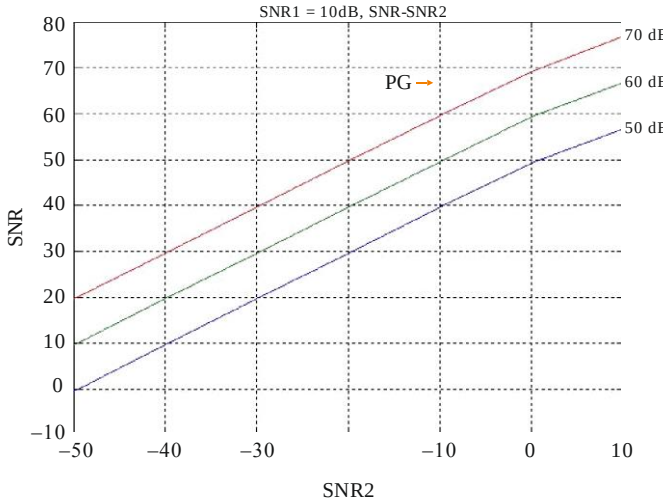

Report SM.2355-A1-03

Typically, the equipment using cross-correlation arithmetic can detect weak signals with about −40 dB snr value if the processing gain is 60 dB. That is to say, it can capture the weak signal with a power spectrum density 40 dB lower than the noise floor.

In practice, the directional horn antenna rotates by a certain angle followed by a cross-correlation process. After rotating 360 degrees, the operator would be able to find the direction of the transmitter when the correlation snr of the both channels (from satellite and from earth station) maximizes, even when the level of the terrestrial signal is too weak to be observed with a spectrum analyser (see Fig. A1-4).

FIGURE A1-4

Peak angle graph

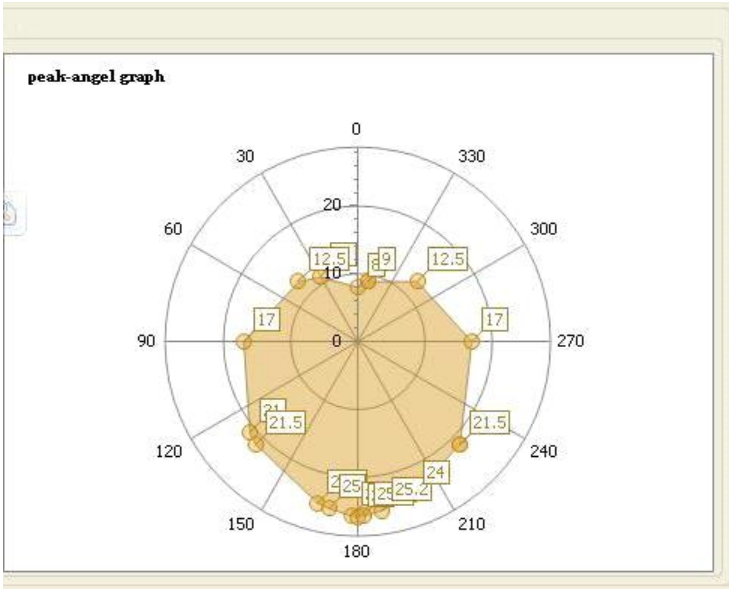

Report SM.2355-A1-0

Alternately, equipment using cyclic auto-correlation based arithmetic can detect weak signals with about −20 dB snr values, correspondingly. Although the performance is worse than cross-correlation based arithmetic, it still exhibits better sensitivity than traditional FFT-based detection algorithm. The diagram is shown in Fig. A1-5.

FIGURE A1-5

Diagram of cyclic auto-correlation application in satellite interference finding

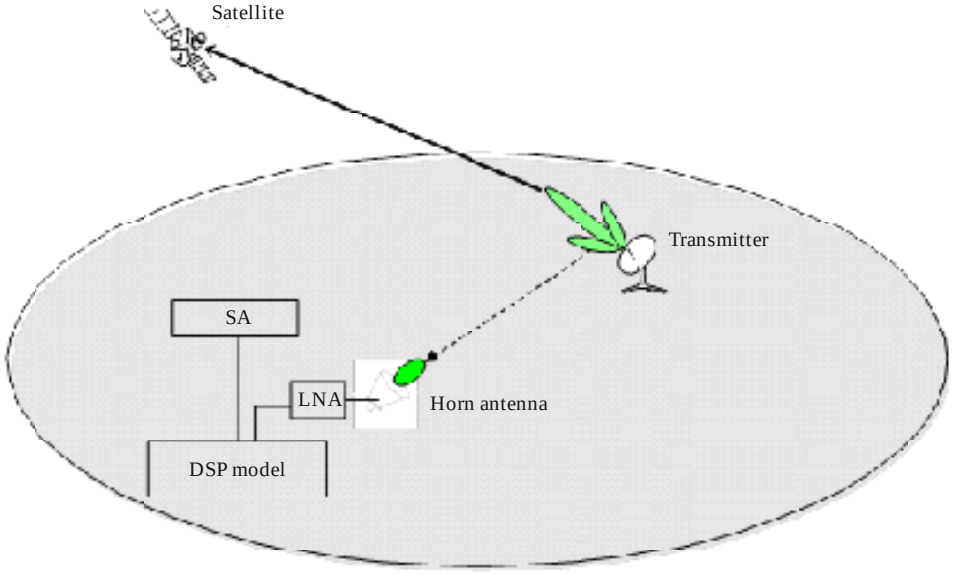

Report SM.2355-A1-05

Comparably, equipment using cyclic auto-correlation based arithmetic can detect weak signals from earth station transmitters several kilometres away, and equipment using cross-correlation based arithmetic can detect weak signals from earth station transmitters several tens of kilometres away; however equipment using a traditional monitoring receiver or spectrum analyser can only detect weak signals from earth station transmitters several hundreds of metres away under certain situations.

A1.2 Strong-signal recovery application in satellite monitoring

GSO satellite network interference happens occasionally due to equipment failure and misoperation. As a general rule, there are two signals working at overlapping frequencies. At this time strong-signal recovery may be applied for interference monitoring and alarming. A brief diagram of this application is shown in Fig. A1-6.

FIGURE A1-6

Diagram of strong-signal recovery application in satellite monitoring

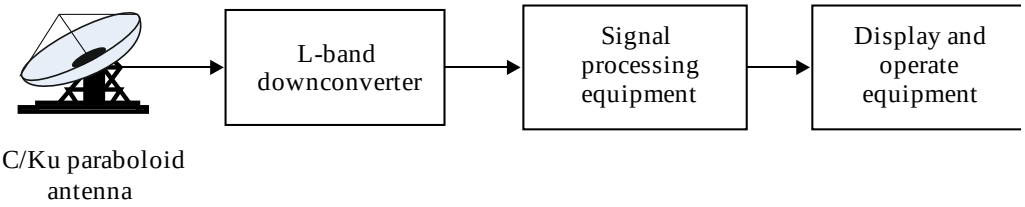

Report SM.2355-A1-0

Here is an example of a strong signal recovery application in GSO satellite network interference separation. The legal signal is in BSS application with QPSK modulation and baud-rate of 26.042 Mbit/s, the interfering signal is a CW signal.

As can be seen in Fig. A1-7 that the spectrum shown as a green line represents the received signal, which can be known as the spectrum of the mixed signal, while the spectrum in blue represents the separated interfering signal. The modulation type and the corresponding modulation parameters are listed in the form below.

FIGURE A1-7

Example of GSO satellite network interference separation

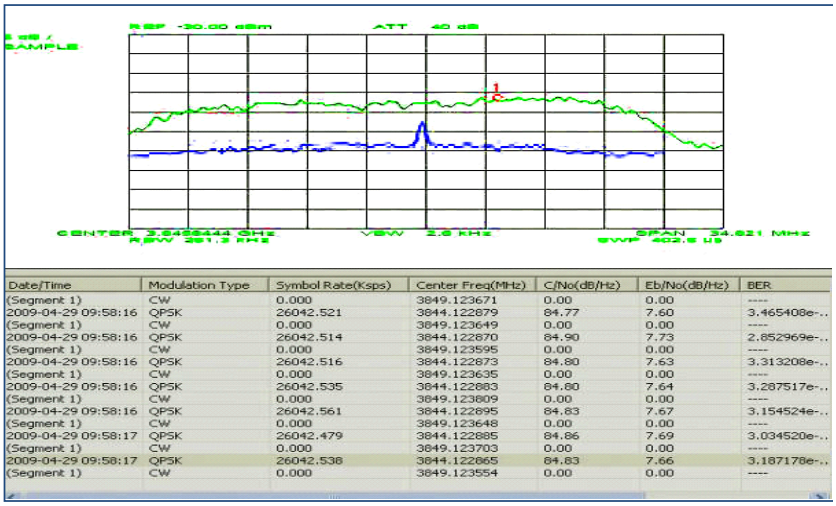

Date/Time	Modulation Type	Symbol Rate(Ksps)	Center Freq(MHz)	C/No(dB/Hz)	Eb/No(dB/Hz)	BER
(Segment 1)	CW	0.000	3849.123671	0.00	0.00	----
2009-04-29 09:58:16	QPSK	26042.521	3844.122879	84.77	7.60	3.465408e-..
(Segment 1)	CW	0.000	3849.123649	0.00	0.00	----
2009-04-29 09:58:16	QPSK	26042.514	3844.122870	84.90	7.73	2.852969e-..
(Segment 1)	CW	0.000	3849.123595	0.00	0.00	----
2009-04-29 09:58:16	QPSK	26042.516	3844.122873	84.80	7.63	3.313208e-..
(Segment 1)	CW	0.000	3849.123635	0.00	0.00	----
2009-04-29 09:58:16	QPSK	26042.535	3844.122883	84.80	7.64	3.287517e-..
(Segment 1)	CW	0.000	3849.123809	0.00	0.00	----
2009-04-29 09:58:16	QPSK	26042.561	3844.122895	84.83	7.67	3.154524e-..
(Segment 1)	CW	0.000	3849.123648	0.00	0.00	----
2009-04-29 09:58:17	QPSK	26042.479	3844.122885	84.86	7.69	3.034520e-..
(Segment 1)	CW	0.000	3849.123703	0.00	0.00	----
2009-04-29 09:58:17	QPSK	26042.538	3844.122865	84.83	7.66	3.187178e-..
(Segment 1)	CW	0.000	3849.123554	0.00	0.00	----

Report SM.2355-A1-0

A1.3 Single-channel ICA application for signal separation

Here is an example of two co-channel BPSK signals separation based on ICA algorithm. The system diagram is shown in Fig. A1-8. The two signals are with the same baud rate and only have a small carrier frequency offset. Based on the ICA algorithm, the signals are separated from the mixed signal, as shown in Fig. A1-9. If the signal-to-noise ratio (SNR) is 10 dB and the signal-to-interference ratio (SIR) is 0 dB, the correlation coefficient between the original and the separated signal could achieve

more than 0.93. It can be seen clearly that the co-channel signals are completely separated. Figures A1-10 and A1-11 give the separation results in terms of a constellation diagram. By changing SNR from 4 dB to 12 dB, the bit error ratios (BERs) of the separated signals are shown in Fig. A1-12. We can see that the BERs are less than 10^{-3} when SNR is larger than 10 dB, which is a very common satellite communication environment.

In another simulation, we treat signal 1 and signal 2 as the desired signal and the interfering signal, respectively. For different SIRs (−10 dB to 10 dB), the BERs of the desired signal are shown in Fig. A1-13. We can see that the desired signal could be correctly abstracted from the mixed signal when SIRs are larger than 0 dB. For low SIRs (less than 0 dB), the interfering signal could be abstracted firstly and cancelled from the mixed signal, and then the desired could be obtained. At present, this co-channel ICA algorithm could only separate two binary digital modulation signals. More robust algorithm for multi-ary modulation signals should be studied.

FIGURE A1-8

Diagram of single-channel ICA application for signal separation

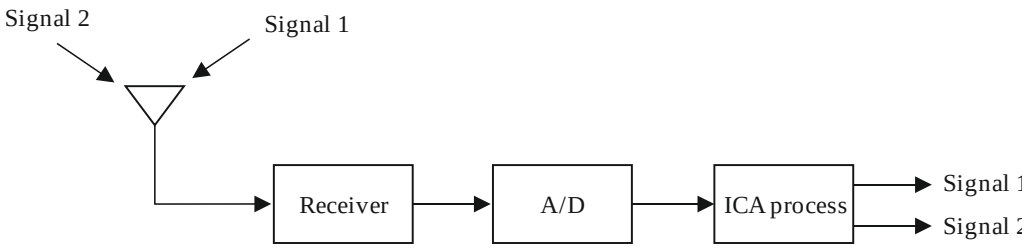

Report SM.2355-A1-0

FIGURE A1-9

Results of separation of two BPSK signals

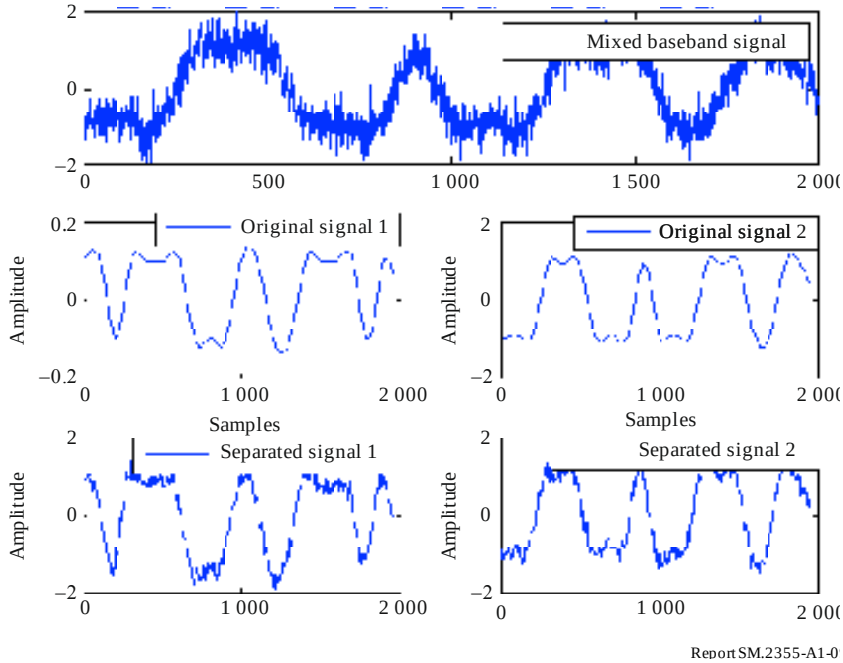

Report SM.2355-A1-0

FIGURE A1-10

Constellation diagram of the mixed signal

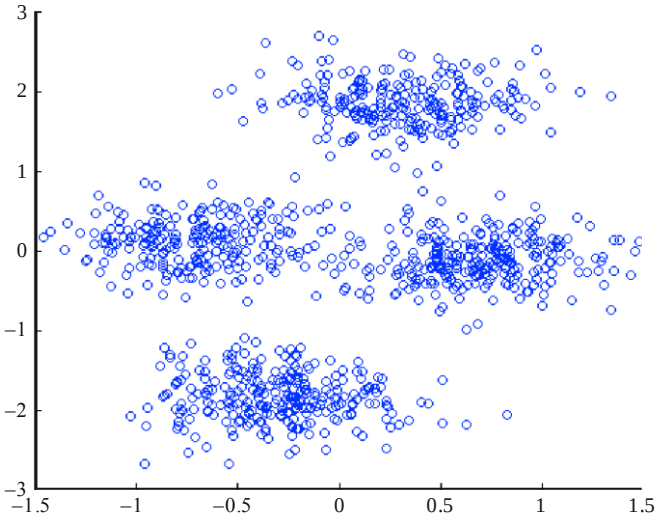

Report SM.2355-A1-1(

FIGURE A1-11

Constellation diagram of the separated signals

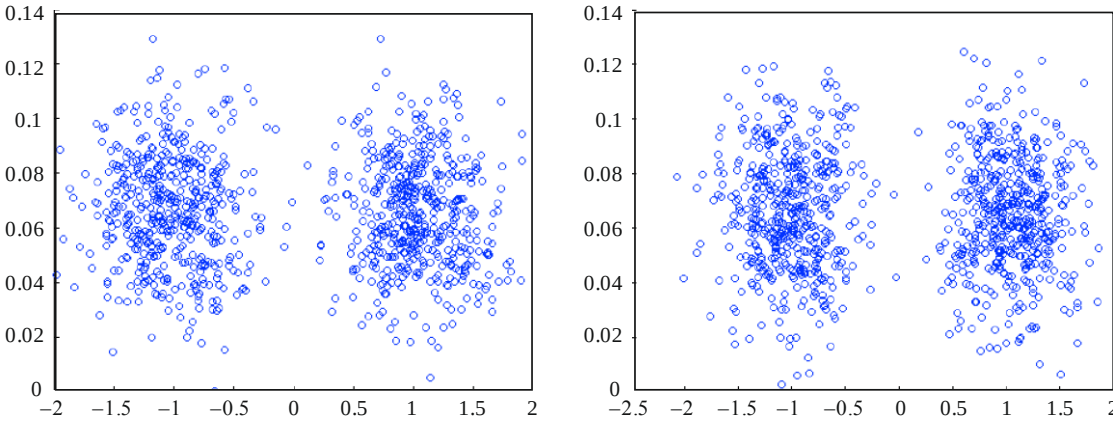

a) Separated signal 1

b) Separated signal 2

Report SM.2355-A1-1

FIGURE A1-12

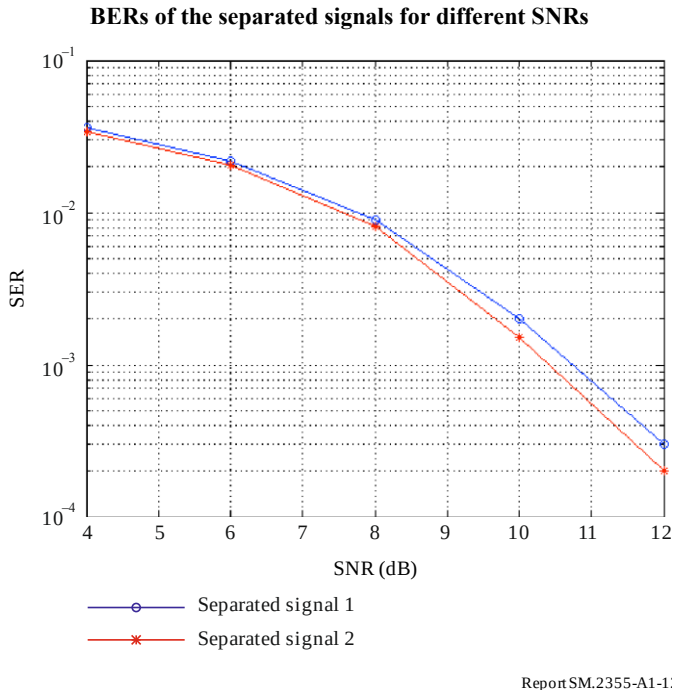

FIGURE A1-13

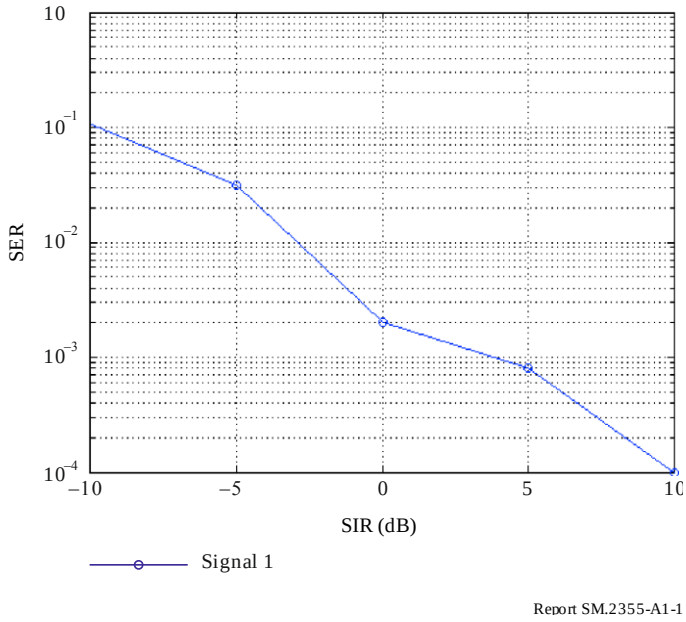

A1.4 Spatial spectrum based beam-forming in HF/VHF monitoring

Spatial spectrum-based beam-forming technology is widely used in HF/VHF monitoring system when it is necessary to listen and locate HF/VHF signals working at overlapping frequencies. A brief structure is shown in Fig. A1-14.

FIGURE A1-14

Diagram of spatial spectrum based beam-forming application in HF/VHF monitoring

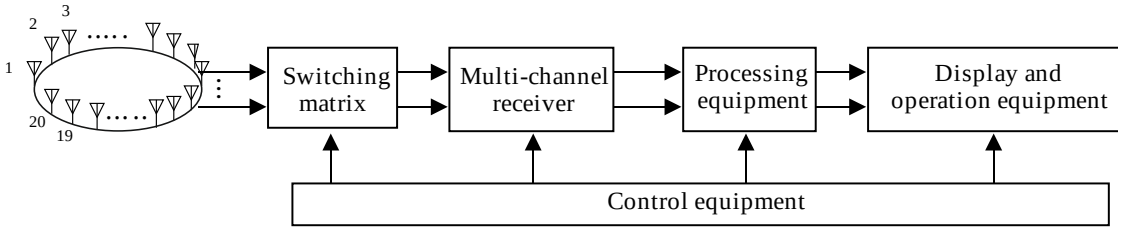

The most common shape of array is the circular array, others are triangle and line arrays. The received signal is transmitted to a multi-channel receiver through a switching matrix. In general, the number of the receiving channels equals that of the antenna arrays. Some processing steps, such as down conversion, filtering, and digitization, are usually completed by the receiver. It is worth noting that each receiving channel should satisfy the consistence in phase and amplitude, otherwise the posterior processing would be ineffective. The processing equipment implements the direction-finding and beaming-forming algorithms, and interacts with the display and operation equipment.

The following content is an example of blind separation of two signals. Both signals are from interphone applications of FM modulation with the same power. Figure A1-15 shows the estimated result of direction of arrival by the MUSIC algorithm. It can be seen clearly that the two directions of 0º and 90º are accurately estimated. The comparison of the original and the separated signal for the desired and undesired signals are shown in Figs A1-16(a) and A1-16(b), respectively. The result shows that both signals are well separated. By calculating *MSE* as the evaluation parameter, which is defined as:

$$MSE = \sqrt{\left(\sum_N \left(S(n) - S_e(n)\right)^2\right) / N}$$

where $S(n)$ and $S_e(n)$ are the original and the separated signal respectively, N is the number of the signal, and the magnitude of *MSE* is around 10^{-3}.

FIGURE A1-15

Results of the direction of arrival estimation

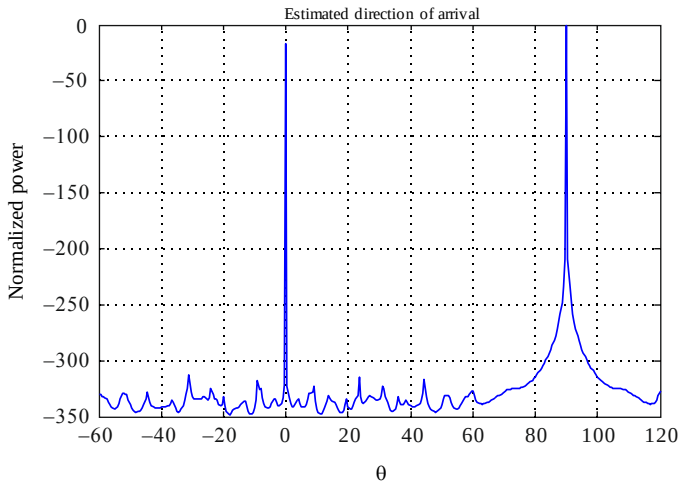

FIGURE A1-16

Comparison between the original and the separated signal

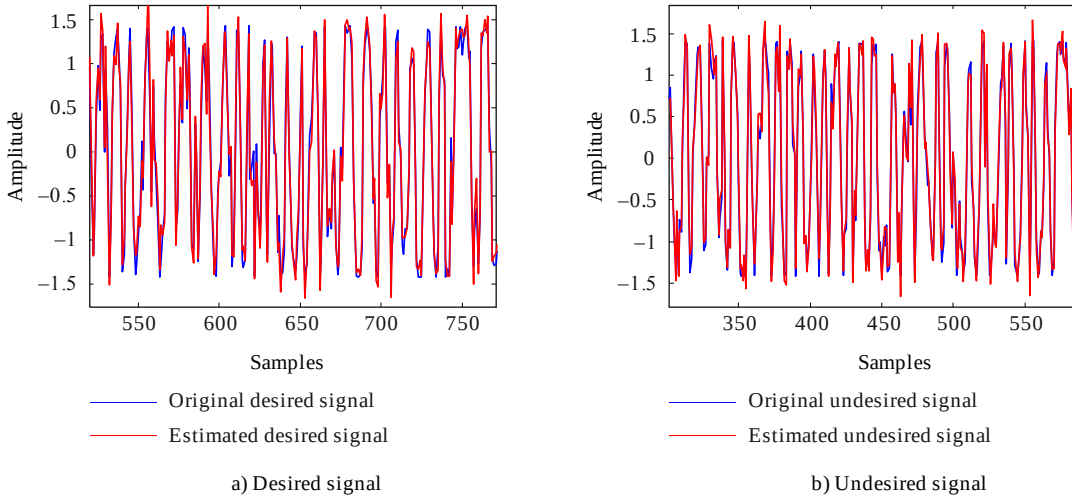

Figure A1-17 shows the evaluation result of the *MSE* ratio under different power ratio between the desired and undesired signals. It can be seen that the power ratio has significant influence on the effect of the separation result. Generally speaking, strong signal outcomes a comparable less *MSE* than that of the weak signal, and shows a better separation performance. As a particular case, the *MSE*s are similar when the two signals have the same power.

FIGURE A1-17

***MSE*s under different power ratios between the desired and undesired signals**

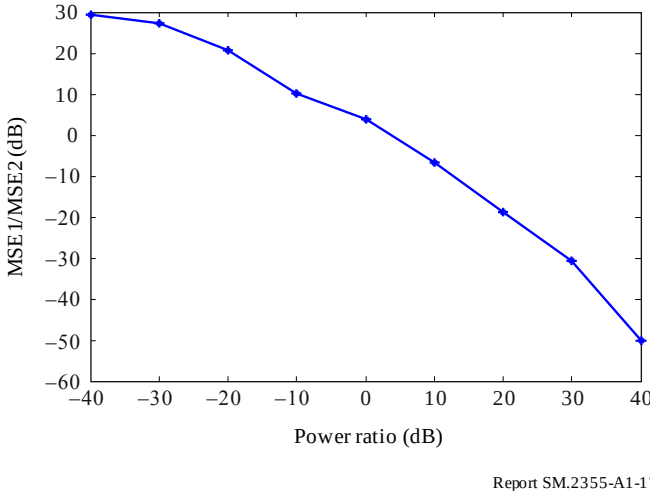

A1.5 Multi-channel ICA application for signal separation

This part introduces the results of evaluation of multi-channel ICA application for interference signal separation using an experimental test bed.

A1.5.1 Details of tests

A signal comprising an interference wave superimposed on a desired signal was transmitted as the test signal, which was then received by an array antenna. The received signal was first A/D converted and then the ICA processing was carried out.

By obtaining the difference between the estimated power ratio (DUR_{est}) of the desired wave and the interference wave which were separated by ICA processing and the set electric power ratio (DUR) of the test signal, the DUR estimation accuracy was evaluated.

Desired to undesired power ratio of the test signal (DUR) = (desired signal power) / (undesired signal power)

Estimated power ratio after ICA processing (DUR_{est})

= (*desired signal power*) / (*undesired signal power*)

DUR estimation accuracy (A) = $DUR_{est} - DUR$

As viewed from the array antenna, the arrival direction of the desired wave is kept fixed, the arrival direction of the interference wave is changed from 5° to 180°, and the change in the DUR estimation accuracy due to changes in DUR for each arrival angle were evaluated.

Figure A1-18 shows a system diagram of the evaluation test.

FIGURE A1-18

System diagram of evaluation test

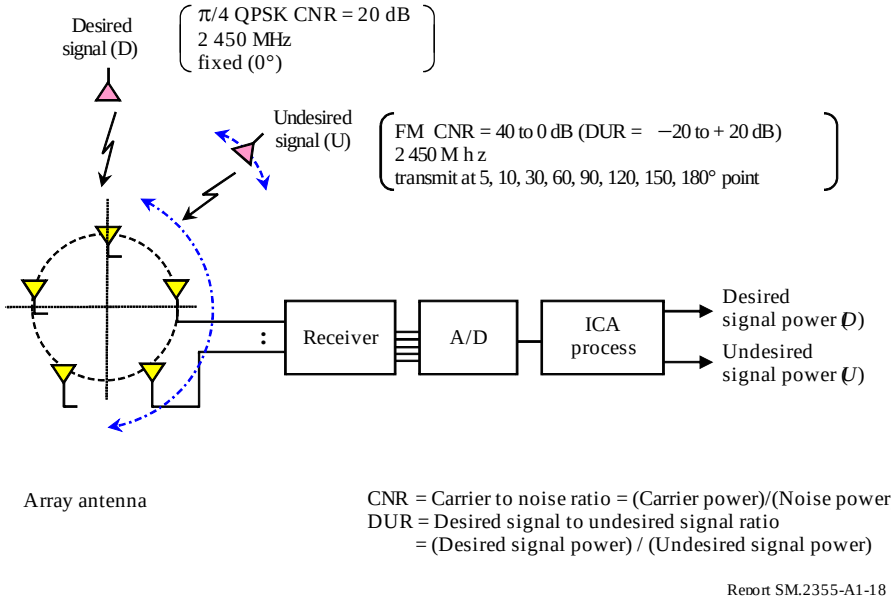

A1.5.2 Test results

A constellation diagram of the received signal before ICA processing and the desired wave and interference wave separated by ICA processing is shown in Fig. A1-19. Furthermore, the measured results of the DUR estimation accuracy in the case of the desired wave π/4 QPSK and the interference wave FM are shown in Fig. A1-20.

In the range of DUR = −15 to +10 dB, it was confirmed that it is possible to estimate the DUR of the interference signal within an accuracy of less than 2 dB.

With the same procedure as this test, we carried out a test in the case of the test signal comprising the desired wave AM and the interference wave FM. Although there was some slight difference in the results, results showed on the whole a similar trend and similar results.

With the same procedure as this test, the results of carrying out tests for antenna aperture diameters showed the trend that the range of DUR that can be measured becomes wider towards larger aperture diameters.

FIGURE A1-19

Constellation diagram of signals separated by ICA

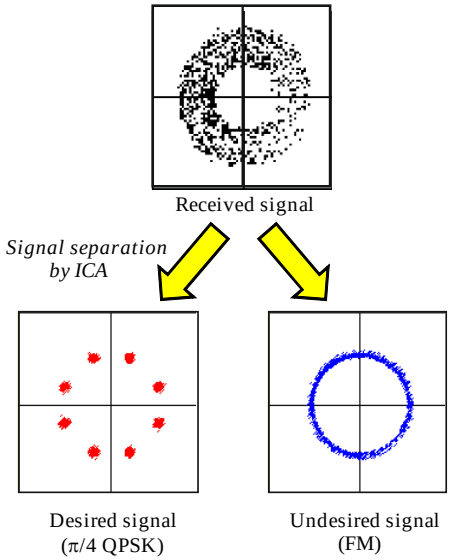

FIGURE A1-20

Accuracy of DUR estimation

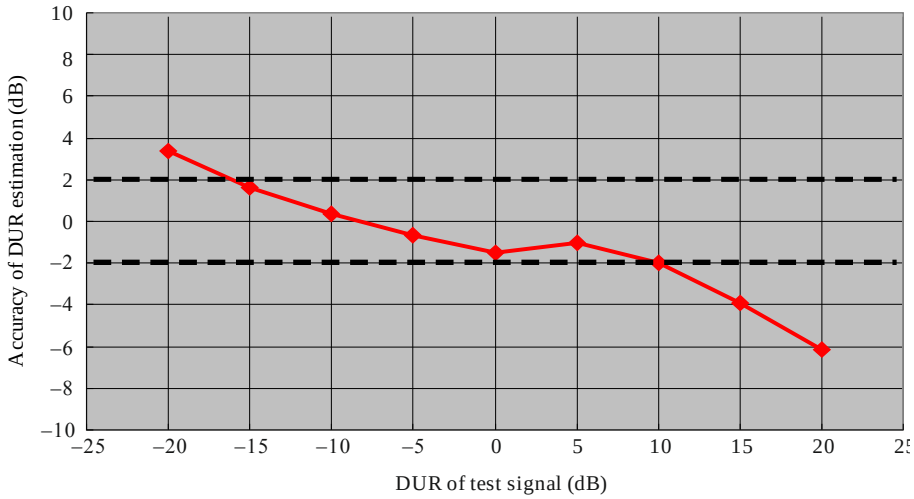

A1.5.3 Interference detection processing

As shown in the results of evaluating the ICA method, this method can estimate DUR with a high accuracy from the signal power ratio after separation. Therefore, it is evident that it is possible to monitor quantitatively and with appropriate timing in actual situations of weak levels of interference in which there is no significant degradation in the communication quality, and in rarely occurring actual cases of interference.

In more specific terms, in a general digital wireless system, even when there is an interference of about *DUR* = 10 dB, by the use of error correction codes, the user does not notice that interference has occurred. Because of quantitatively estimating the DUR using the ICA method, it is considered possible to take countermeasures before a significant degradation occurs in the communication quality.

As shown in Fig. A1-21, in this method, in the range of *DUR* = −15 to +10 dB, since it is possible to measure the signal level with an accuracy of ±2 dB, within this DUR range, it is expected to be possible to detect the presence of an interference with a good accuracy.

By setting the threshold value for detecting the presence of an interference by referring to the *C/N* (= *DUR*) required by the communication system of the desired wave, it is possible to output an alarm or make a record automatically in synchronization with the interference detection timing.

A1.6 GSM base station geolocation

It is necessary to locate GSM base stations when there is interference between different GSM network operators, or there is demand on GSM network coordination at border areas. Monitoring stations can be used to differentiate GSM base stations belonging to different GSM network operators by utilizing traditional DF and geolocation method. However, it is easier to implement such a task by decoding GSM signals and extracting information, such like GSM network operator, Cell Global Identification (CGI), etc.

CGI is a unique number used to identify the GSM base station the user equipment is connected to. The Cell Global Identification is the concatenation of the Location Area Identification and the Cell Identity. The brief diagram of extracting CGI is shown in Fig. A1-23.

FIGURE A1-21

Diagram of extracting cGI

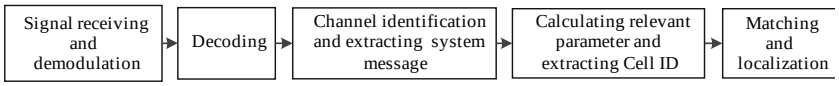

Report SM.2355-A1-2

GSM signal should be demodulated and decoded firstly after it is received by a monitoring station receiver. Then the special channel should be identified and the system message should be extracted from it. Position of GSM base station can be known after matching relevant parameter and cell ID with database. In combination with AOA method, a mobile monitoring station can locate accurate position of GSM base stations in one area by planning appropriate monitoring route.

Annex 2

Examples of the application of combined geolocation

A2.1 Hybrid AOA/TDOA

In general, there is no single method such as the ones based on measuring time difference of arrival (TDOA) and angle of arrival (AOA) that will provide accurate location estimation under all circumstances. Each method has its own advantages and limitations in terms of location accuracy.

TDOA location methods generally provide better location accuracy for wideband signals than the AOA-based location method. However, the TDOA-based methods require relatively more stations than the AOA-based methods to perform location of emitters. For instance, the TDOA-based methods require at least three properly distributed stations for location. The AOA methods, on the other hand, require two stations for location. However, a small error in the angle measurements will result in a large location error if the station is far away from the transmitter. Therefore, to achieve better location accuracy, a combination of two or more location schemes should be considered in order to complement each other.

The location is performed by processing the information available from each station, including AOA measurements, TDOA measurements and station position information. Combining the AOA method with the TDOA method (called hybrid AOA/TDOA) can assist in eliminating location ambiguity associated with TDOA alone and can enhance location accuracy. This is illustrated in Fig. A2-1. A more complete discussion of Hybrid AOA/TDOA methods is contained in the ITU Handbook on Spectrum Monitoring, Edition 2011, Chapter 4.7.3.6.

FIGURE A2-1

Improved results based on AOA/TDOA combined techniques

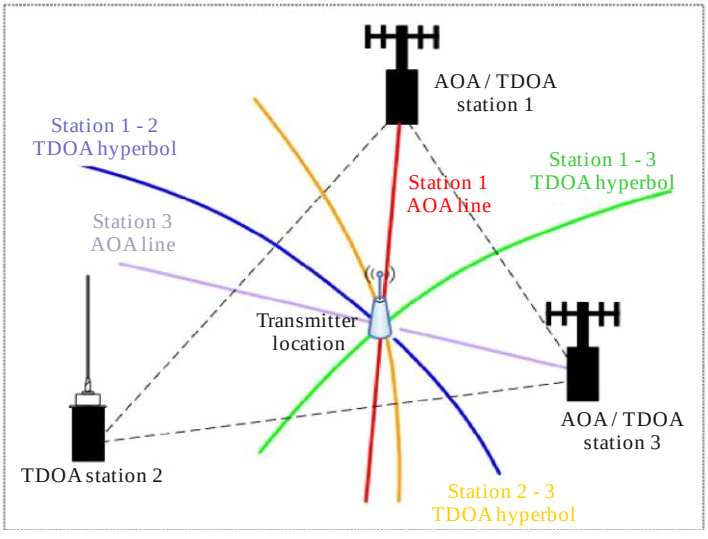

Report SM.2355-A2-01

Using POA techniques generally works best at specific distances from the transmitter depending on power and what clutter and other signal disturbances (e.g. absorbers) are in the area. This is especially important since these techniques typically use line-of-sight propagation models, working as a combined geolocation technique along with AOA and TDOA. This is illustrated in Fig. A2-2.

FIGURE A2-2

Combined geolocation

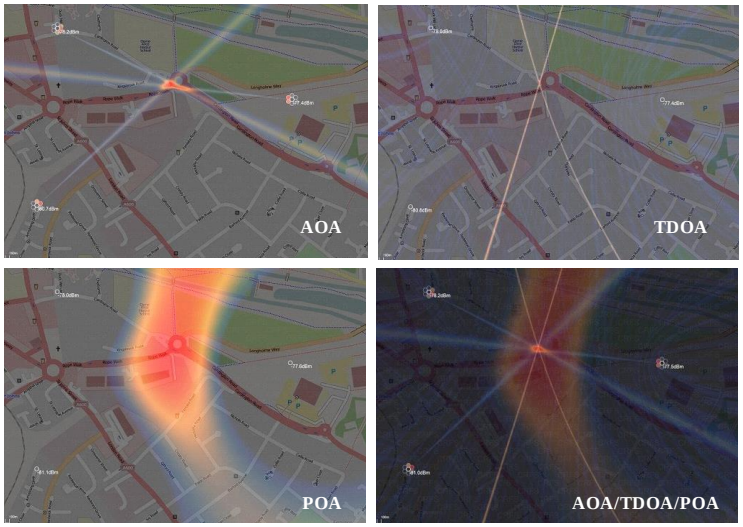

Report SM.2355-A2-0

A2.2 Hybrid TDOA/GROA

A2.2.1 Introduction

Grid monitoring network technology is one of the technologies which can spatially describe and display unknown radio emitters and assess spectrum resources using remote distributed RF intelligent monitoring nodes. The grid monitoring network technology meets the challenges of modern spectrum usage and efficiency requirements of managing spectrum resources for the metropolitan environment. The components and architecture of this type of system differentiate it from other systems with more traditional angle-of-arrival direction-finding (DF) systems, which can be more complex, expensive and often used in large-scale scenarios.

China commissioned a study into the design of a grid monitoring network that could be deployed in large numbers to automatically detect, identify and locate the source of interfering radio signals over a large part of a metropolitan area in China. In June, 2012, the experimental programme was launched, which covers over 75 square kilometres in the downtown area of Shanghai with 46 networkable nodes, as shown in Fig. A2-3. More than 50 researchers and engineers joined this programme, which is the first experimental area to explore methods for metropolitan area radio monitoring with a large number of cost-effective nodes in China. The experimental programme was implemented in June 2013. The field test was conducted by 16 test participants from third parties in August 2013. The experimental network had been running in the test phase for nearly one year by 2014.

FIGURE A2-3

The grid monitoring network with 46 nodes

Report SM.2355-A2-0

A2.2.2 Architecture of grid monitoring network

The grid monitoring network is a typical mesh network that supports dynamic networking and scalable structure. The structure of the grid monitoring network in the programme consists of three layers, as shown in Fig. A2-4:

– the sensor layer: including all the cost-effective networkable nodes (bi-conical antenna, sensor and GPS antenna);

– the middle service layer: consisting of the sub-centre servers with several grids, to organize and allocate the monitoring tasks to the sensors;

– the monitoring centre layer: including all the software applications such as spectrum monitoring, locating and data mining.

FIGURE A2-4

The architecture of the grid monitoring network

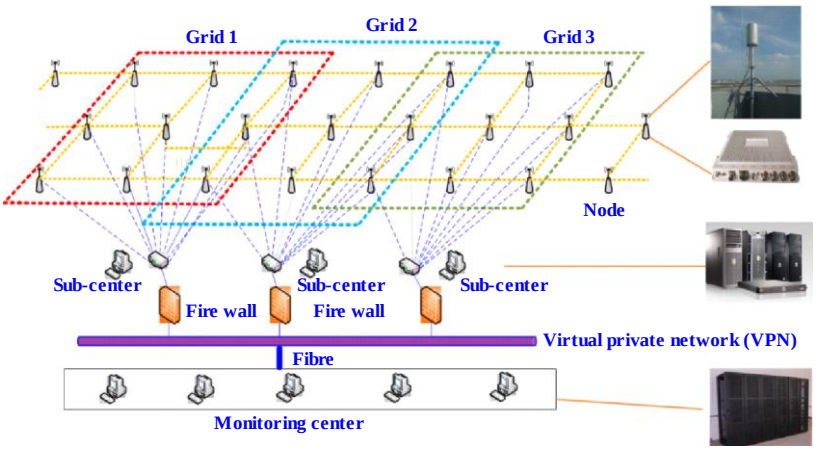

Report SM.2355-A2-0

The grid monitoring network process flow is shown in Fig. A2-5.

FIGURE A2-5

The grid monitoring network process flow

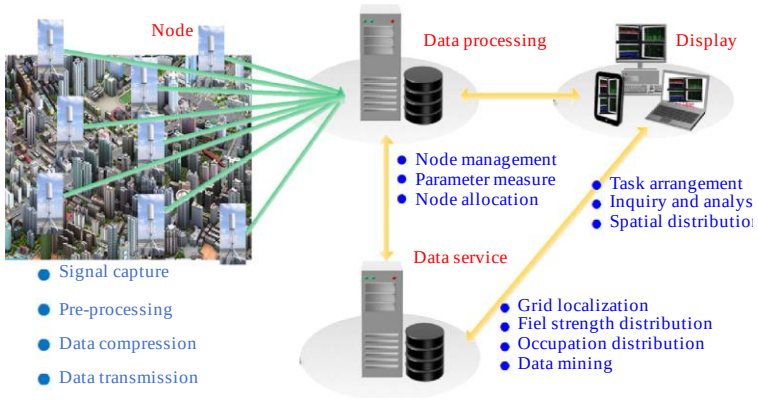

Report SM.2355-A2-0

A cost-effective networkable node, such as that shown in Fig. A2-6, is the key component in the grid monitoring network. It is significantly different from the direction finding node, which is often multi-channels and quite expensive. Therefore, the grid monitoring network costs may be significantly lower by utilizing signal correlation methods, depending on the size of the monitoring area and hence the number of required nodes. Investigation of cost is of great importance for developing countries with a limited budget, and to metropolitan areas with large number of monitoring nodes.

FIGURE A2-6

Cost-effective networkable RF sensor and bi-conical antenna

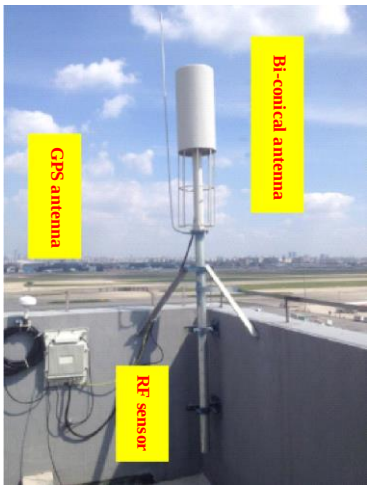

Report SM.2355-A2-0(

A2.2.3 System functionalities

A2.2.3.1 Intercept weak signal

The monitoring performance has been tested based on the mounted sensors from the grid monitoring network. The field test has been carried out as long as 19 days in the coverage areas by 16 testers from third parties.

The minimum emission power level of the “target” emitter (emitter to be detected) is defined as signal-to-noise ratio (SNR) ≥ 6 dB in the receiver for different frequencies (including 115 MHz, 320 MHz, 575 MHz, 965 MHz, 1 300 MHz, 1 700 MHz, 2 600 MHz) and different bandwidths (including 12.5 kHz, 25 kHz, 100 kHz, 200 kHz, 1.25 MHz, 8 MHz), the result is shown as Table A2-1.

TABLE A2-1

Detection probability for different power of the emitter (131 measurements)

	Power emitter ≥ 1W	**Power emitter ≥ 0.1W**	**Power emitter ≥ 0.05W**
Detection measurements (SNR ≥ 6 dB)	128	114	92
Detection probability (SNR ≥ 6 dB)	97.7%	87%	70.2%

A2.2.3.2 Hybrid geolocation

The grid geolocation (hybrid TDOA and GROA: time difference of arrival and gain ratio of arrival) performance has been tested.

The gain ratio of arrival (GROA) is an energy-based passive method that can be used to estimate the positions of the source from the multiple sensors. This method does not require accurate time synchronization between sensors. A particular value of the GROA estimate defines a circle between the two receivers on which the radio transmitter may exist.

The time difference of arrival (TDOA) technique is one of the most promising position location techniques for wireless communication systems. TDOA techniques are based on estimating the difference in the arrival times of the signal from the source at multiple receivers. A particular value of the time difference estimate defines a hyperbola between the two receivers on which the radio transmitter may exist, assuming that the source and the receivers are coplanar, shown as Fig. A2-7.

FIGURE A2-7

Schematic diagram of the hybrid GROA/TDOA geolocation techniques

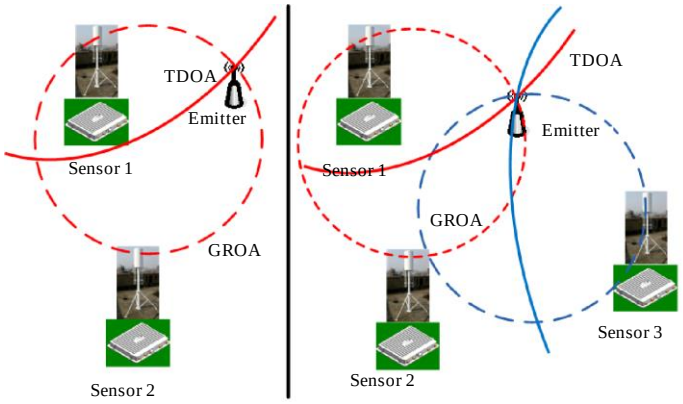

The test result shows that the proportion of typical errors (deviation between the true location and estimated one) less than 300 metres is about 82.3% in the 402 measurements. The proportion to the typical value of the grid locating deviations less than 100 metres is about 24.9%. Table A2-2 shows the parameters of the testing transmitter.

Specifically, the grid monitoring network can distinguish and geolocate two signals operating on the same frequency simultaneously because of the grid resolution. For a test example with two emitters with following parameters as frequency 220 MHz, bandwidth 50 kHz, power 1 W and QPSK modulation, the grid monitoring network gives high spatial resolution for simultaneous emitters operating at different distances apart from each other (in Figs. A2-8, A2-9 and A2-10), except in the case where the two emitters are in the same grid (in Fig. A2-11).

TABLE A2-2

Hybrid geolocation test parameters

Parameters	Value
Frequency (MHz)	115, 320, 575, 965, 1 300, 1 700, 2 600
Bandwidth (Hz)	12.5K, 25K, 100K, 200K, 1.25M, 8M
Modulation	AM, FM, FSK, QPSK, MSK, QAM
Power	1W

FIGURE A2-8

Co-frequency signals spatial separation (Emitter pairwise distance is 7.2 km)

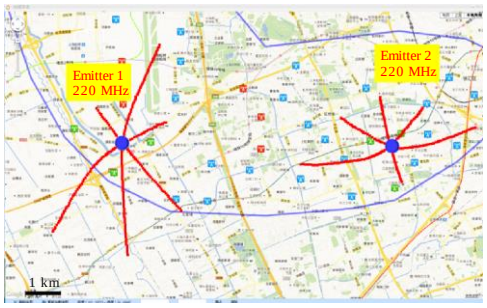

Report SM.2355-A2-0

FIGURE A2-9

Co-frequency signals spatial separation (Emitter pairwise distance is 5.7 km)

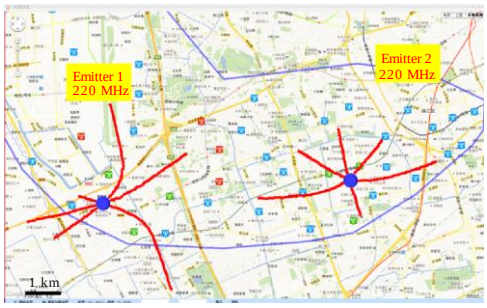

Report SM.2355-A2-0

FIGURE A2-10

Co-frequency signals spatial separation (Emitter pairwise distance is 4.1 km)

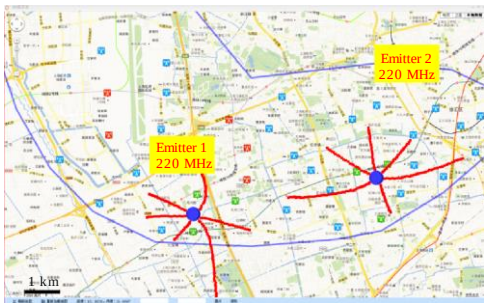

Report SM.2355-A2-1

FIGURE A2-11

Co-frequency signals spatial separation (Emitter pairwise distance is 0.6 km)

Report SM.2355-A2-1

A2.2.3.3 Field-strength distribution

Field strength can be measured by all nodes simultaneously, and the distribution of the channel in the coverage area can be detected and calculated by the grid monitoring network by real-time data interpolation. The distribution is computed according to the field strength detected by all the sensors, and the monitoring data will be merged in real-time. Two examples are presented below for the case of one 3 W emitter and two 3 W emitters operating simultaneously.

FIGURE A2-12

Field strength distribution (Frequency 140.5 MHz, bandwidth 12.5 KHz, FM, power 3W)

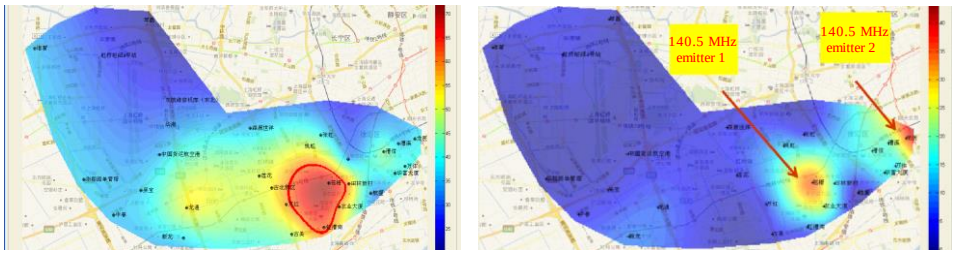

a) Single walkie-talkie test b) Double walkie-talkie test

Report SM.2355-A2-12

Figure A2-12 shows that the radio propagation is anisotropic apparently in metropolitan environments, which is different from the theoretical isotropic propagation models. The two emitters operating on the same frequency can be spatially distinguished clearly by the grid monitoring network. Here, the distance between the emitters is less than 3 km. However, this is difficult to accomplish using a more conventional DF network system in the metropolitan environment.

A2.2.3.4 Geographic occupation and electromagnetic radiation distribution

Traditional spectrum occupancy is often a single value for one place. Also, it is not easy to describe clearly how spectrum resources are used. The grid monitoring network can provide details about the spectrum occupation spatially. The spectrum occupancy can be measured by all the nodes simultaneously in Fig. A2-13 (Freq = 400.5 MHz, BW = 12.5 kHz, FM, power = 3 W).

With the raw spectrum data within the grid monitoring network, the electromagnetic radiation geographic distribution can also be described in the covered areas, as shown in Fig. A2-14. The frequency band is 30 MHz to 3 000 MHz, and the unit of the electromagnetic radiation is power density in uW/cm^2.

FIGURE A2-13

Geographical spectrum occupancy distribution

Report SM.2355-A2-1

FIGURE A2-14

Electromagnetic radiation distribution

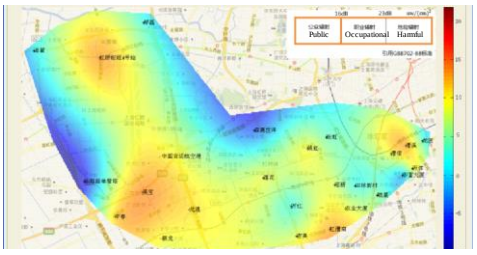

Report SM.2355-A2-14

A2.2.4 Conclusion

The grid monitoring network with cost-effective nodes has the ability to intercept the weak signals, to provide the details of radio monitoring and to describe the spectrum spatial distribution for the metropolitan environment, so it is meaningful and effective in identifying the spectrum spatial distribution and the location of the interference sources quickly.